OBJECT- BASED LAND USE/LAND COVER CHANGE DETECTION USING SPATIO -TEMPORAL IMAGES – A CASE STUDY IN METROPOLITAN CITY OF ISTANBUL, TURKEY

Taskin Kavzoglu (1), Elif Ozlem Yilmaz (1), Hasan Tonbul (1)

[1]Gebze Technical University, Geomatics Engineering Department, 41400, Gebze-Kocaeli, Turkey
Email: kavzoglu@gtu.edu.tr; eoyilmaz@gtu.edu.tr; htonbul@gtu.edu.tr

KEY WORDS: Land degradation, image segmentation, change detection, OBIA.

ABSTRACT: Due to the high industrialization and corresponding increase in population, a significant number of housing request was witnessed in the last several decades in metropolitan city of Istanbul, Turkey. As a result, a significant amount of land degradation and environmental change has occurred, particularly in the outskirts of the city. According to the Turkish Statistical Institute's (TUIK) report for 2018, Istanbul is the most populous city in Turkey, reaching to 15 million. For the rise of human needs, new transportation structures including roads, airports and bridges have been lately built in the city. Hence, the construction of built-up areas has led to an essential fluctuation in land use/land cover (LULC) in the region. The construction of the Istanbul Grand Airport (IGA) (2014-2018) and the Yavuz Sultan Selim Bridge (2012-2016) have affected the wetlands and forests directly affecting ecological habitat. In this study, two satellite images acquired in July 2013 and April 2018 from Landsat 8 OLI/TIR were employed to investigate the LULC changes in the city. In this context, six main LULC classes namely, water, road, bare soil, urban area, forest and agriculture were determined. The five-year period of change detection of city was performed by using object-based image analysis (OBIA) using multi-resolution segmentation algorithm. The LULC types from the created image segments were determined by using spectral indices, mean, minimum, maximum, standard deviation, brightness and maximum difference of spectral bands. In the classification phase, the nearest neighborhood classifier was applied for producing LULC thematic maps using the multi-temporal images. In parallel to the construction of the IGA (new Istanbul airport) and Yavuz Sultan Selim Bridge, a noteworthy increase in urbanization was observed. Particularly, the area of road class has vastly expanded on a spatial basis, almost doubled in size. Another important finding is that acreage of land water bodies decreased about 500 ha due to the construction of IGA on wetlands and marshlands. Results showed that the study site was subject to approximately 24% LULC change, and the highest change occurred between bare soil and forest classes, corresponding to 5% transition between these classes.

1. INTRODUCTION

Large and metropolitan including Istanbul have been constantly expanding over the years and continuous degradation in the urban structure has been observed. Istanbul, the most populous city in Turkey, presents rich ecosystem in many respects. In parallel with the increase in population, industrial and social areas have increased in the city and considerable changes have occurred in urban areas. Therefore, the changes and degradation in urban lands need to be controlled and monitored periodically. Moreover, rapid changes observed in land use/land cover (LULC) due to unplanned urban growth have to be analyzed in detail by the decision-makers.

Remote sensing techniques are used to observe and identify changes on earth surface and generate high accuracy maps using geo-information obtained from satellite imagery. In particular, production of LULC maps are among the most widely used approaches to extract information about the Earth's surface. Land use demonstrates how the humans use the Earth's surface for their activities such as settlement, agriculture, transportation and development. On the other hand, land cover indicates the physical properties such as water, grass, forest on the landscape (NOAA, 2009). LULC classes can be changeable in some regions related to human activity, so these changes should be studied thoroughly.

Pixel and object-based classifications are the two main approaches for producing LULC maps at different scale using the remotely sensed imagery (Adam, 2016; Linli, 2008; Wu, 2014). In general, traditional pixel-based approaches deals with only spectral information, whereas object-based approaches consider not only spectral information but also texture, shape and size information (Kavzoglu, 2018). By means of object-based classification, the classification of the land surface of Earth is easier than the other methods (Boyaci, 2017). Object-based Image Analysis (OBIA) has been a developing method and there are recent studies which use object-based classification methods to create LULC maps in change detection analysis. (Listner, 2011; Ma, 2016). There are many studies demonstrated that

OBIA provides better accuracy than pixel-based classification (Kavzoglu, 2016; Hussain, 2013; Myint, 2011). OBIA classification categorizes group of pixels depending on the spatial connection with the neighbor pixels using their relevant properties (Walter, 2004; Chen, 2018; Kavzoglu, 2018) OBIA consists of two steps, namely, segmentation and classification. Segmentation is the first and fundamental step of OBIA. Multi-resolution segmentation (MRS) is most commonly used in the literature (Kavzoglu, 2017). The MRS method is managed by three user-defined parameters: scale, shape and compactness.

The main purpose of this paper is to determine LULC changes in Istanbul metropolitan city within the five-year period (2013-2018) using object-based change detection technique. For this purpose, multi-temporal Landsat 8 OLI imagery was used as a main data source. The images were classified using object-based (OBIA) approach to produce LULC maps and then the resulting maps from different times (2013-2018) were compared with each other. The multi-resolution segmentation, a popular segmentation technique available in eCognition software, was used to perform segmentation processes in this study.

2. STUDY AREA AND DATA

The study area covers approximately 2,500 km2 (4,500 pixel by 2,500 pixel) land located in Northern part of Istanbul in Turkey (Figure 1). The study area contains Yavuz Sultan Selim Bridge, which is located in the north of Istanbul near the Black Sea entrance of the Bosporus and Istanbul Grand Airport (IGA) situated on near the Black Sea coastline in the European continent is also located in the study area. The construction of IGA was started in 2014 and finished in 2018. The study area comprises heterogeneous LULC structure; including six major classes namely, water, urban area, road, bare soil, forest and agriculture.

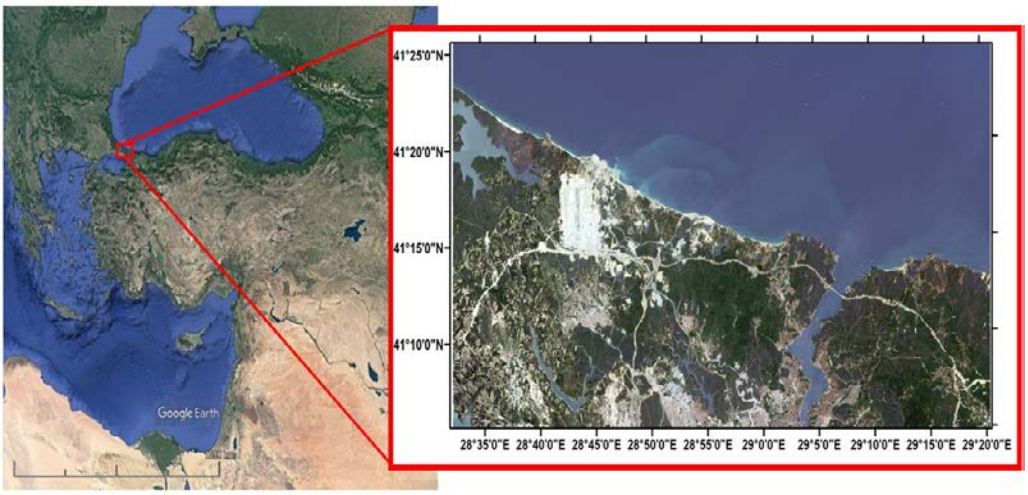

Figure 1. The study area, city of Istanbul, Turkey.

Two Landsat 8 OLI images acquired on 30 July 2013 and 23 April 2018 were downloaded from United States Geological Survey (USGS) Earth Explorer website to analyze the LULC changes occurred in the study site. Landsat images consist of eight spectral bands with spatial resolution of 30 meters and one panchromatic band with spatial resolution of 15 meters. Thermal bands were not considered due to their low spatial resolution and poor contribution to identification of LULC classes (Table 1).

Table 1. The features of Landsat 8 OLI/TIR bands.

Bands	Description	Spectral Resolution (µm)	Spatial Resolution (m)
B1	Violet- Deep Blue	0.43-0.45	30
B2	Blue	0.45-0.51	30
B3	Green	0.53-0.59	30
B4	Red	0.64-0.67	30
B5	Near Infrared	0.85-0.88	30
B6	Shortwave Infrared	1.57-1.65	30
B7	Shortwave Infrared	2.11-2.29	30
B8	Panchromatic	0.50-0.68	15
B9	Cirrus Cloud	1.36-1.38	30

It should be stated that all analyses conducted for object-based classification, accuracy assessment and change detection were carried out using ENVI (v.5.0), MATLAB (R2016a), ArcGIS (v.10.0) and eCognition (v.9.2) software packages.

3. METHODOLOGY

Orthorectified Landsat 8 OLI images were downloaded from USGS website and then pre-processing steps (i.e., resampling, layer stack, dark subtraction and pan-sharpening using Gram-Schmidt) were applied using ENVI software. The processing stage of this study consists of four main parts, which are preprocessing, classification, accuracy assessment, change detection analysis. The processing stages are shown in flowchart (Figure 2).

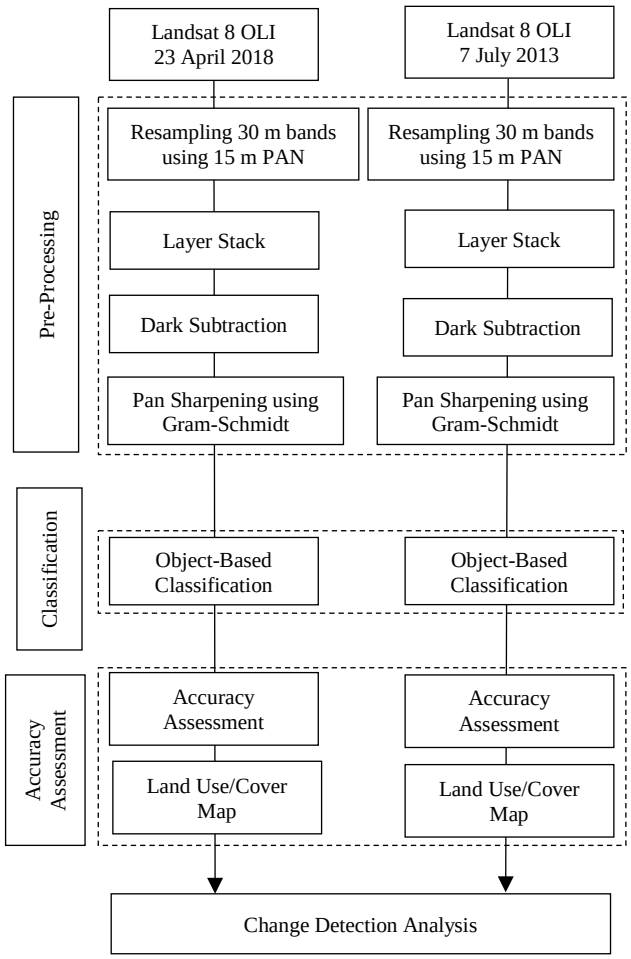

Figure 2. The flow chart of the methodology adopted in this study.

In the pre-processing step, the Landsat 8 images were subsetted considering the extent of the study area. The radiometric corrections of the images were carried out using dark subtraction method to eliminate the unwanted impact of atmosphere from satellite images by subtracting a pixel value that demonstrates a backdrop mark from every band carried out data set (ESRI, n.d.). The pan-sharpening analysis was computed using the popular Gram-Schmidt method. The purpose of this pan-sharpening is to convert low-resolution images to high resolution image to detect LULC classes more precisely (Harris Geospatial, n.d.). Thus, 30-meter resolution bands were converted to 15-meter resolution using the spatial information of the panchromatic band.

In segmentation process, multi-resolution segmentation was performed by using the same segmentation parameters for the satellite images. This step greatly affects the accuracy of the LULC maps. In the classification process, brightness, standard deviation, maximum difference, minimum, maximum, ratio and mean values of all bands and widely used spectral indices (NDVI, NDWI, SAVI, NDBI and BU) were considered. Totally, 33 object features were used, and description of the features are given in Table 2.

Table 2. Definition of the object attributes.

Object Attributes	Definition
BU	Built-up Index
NDVI	Normalized Difference Vegetated Index
NDWI	Normalized Difference Water Index
NDBI	Normalized Difference Built-up Index
SAVI	Soil-adjusted Vegetation Index
Pixel Based Ratio (Definiens, 2007)	The ratio of mean intensity of image object to brightness
Pixel Based Min. Pixel Value (Definiens, 2007)	The minimum pixel value of chosen image objects
Pixel Based Max. Pixel Value (Definiens, 2007)	The maximum pixel value of chosen image objects
Brightness (Definiens, 2007)	The average valuation of the image objects
Max. Difference (Definiens, 2007)	Difference between min. and max. value of image object values
Mean (Definiens, 2007)	The mean value of the chosen image objects
Standard Deviation (Definiens, 2007)	The standard deviation of the chosen image objects

Afterwards, classification using nearest neighborhood method and accuracy analysis stages was performed. The stage of accuracy assessment has a significant role in the evaluation of the classification results. Confusion matrix is commonly used methods in this stage. Also, the producer's and user's accuracy were calculated.

4. RESULTS

In this research, the satellite images were segmented using multiresolution segmentation parameters in order to perform object-based classification. In segmentation process, multi-resolution segmentation was conducted using the same parameters for the selected satellite images. Scale, shape and compactness parameters are used in multiresolution segmentation process to create homogeneous segments using color, texture and shape properties. They were determined in eCognition software by trial and error approach, as used in many studies in the literature (Chen, 2012; Anders, 2011; Stow, 2007). In parameter setting, Scale=50, Shape=0.1 and Compactness=0.7 values were selected. For 2013 and 2018 Landsat datasets, 277,701 and 274,660 segments were created, respectively. It should be also noted that all bands were equally weighted during the segmentation process. The training areas of the study site were determined as homogeneous as possible for all LULC classes based on the spectral characteristics of the region. Segmented image objects of 2013 and 2018 imagery were classified using traditional nearest-neighbor classifier. The similar number of random test data in the study area was selected for each class to assess the accuracy of the LULC maps. High-resolution images and Google Earth images were used to collect test data for 2013 and 2018 LULC maps. Subsequently, the accuracy assessment was carried out. The user's, producer's and overall accuracies were calculated using the confusion matrix approach (Table 3). The overall accuracies for 2013 and 2018 data sets were calculated as 85.68% and 86.36%, respectively. It was observed that the highest user's accuracies were computed for water class as 100% for both images. It should be also noted that the lowest user's accuracy was calculated for agriculture class as 73.00% for 2018 image and road class for 2013 image (Table 3).

Table 3. Classification of accuracy assessment.

	2013 LANDSAT 8 OLI		2018 LANDSAT 8 OLI	
Class Name	**Producer`s (%)**	**User`s (%)**	**Producer`s (%)**	**User`s (%)**
Water	98.77	100	100	100
Agriculture	81.01	80.65	92.21	73.24
Forest	98.09	97.40	82.09	99.60
Urban	76.83	90.55	67.78	91.65
Road	95.76	63.20	96.03	77.92
Bare Soil	70.92	82.30	91.38	75.75
Overall Acc.	85.68 %		86.36 %	

The results of object-based classification from 2013 and 2018 were presented using LULC maps in Figure 3. The LULC class covering the largest area in the study area is water class, the LULC class covering the least area is road class. As can be seen from the figure that some LULC classes (e.g., road and urban - agriculture and bare soil) were confused by the classifier due to the resolution of imagery and spectral similarity of some particular LULC classes.

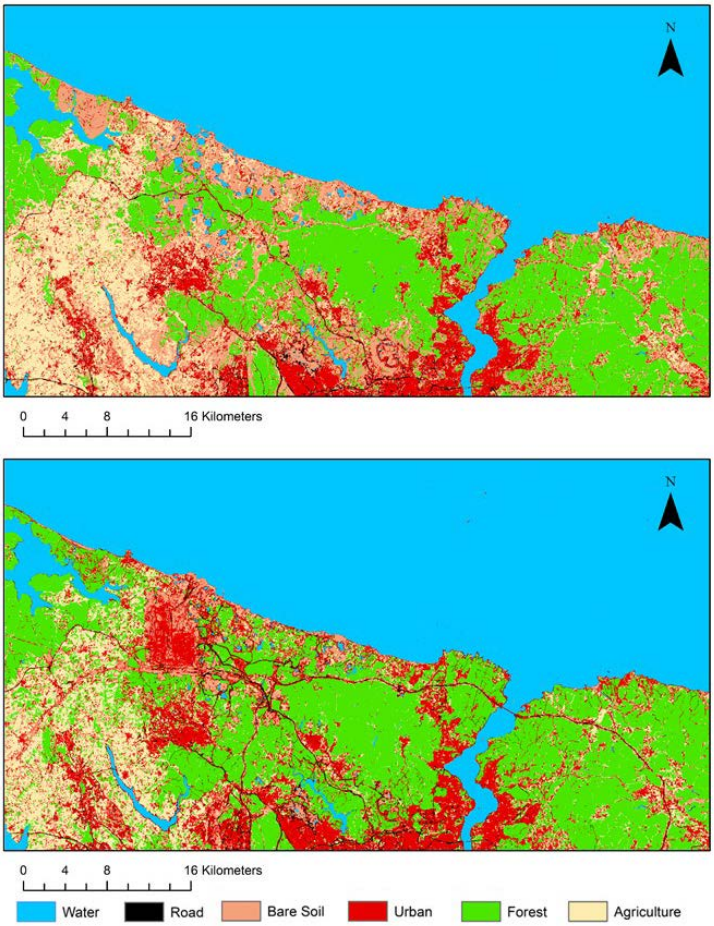

Figure 3. The object-based classification results for 2013 (upper) and 2018 (below).

The change detection analysis was carried out using the classified thematic maps. Table 3 shows the change detection analysis of multi-temporal images considering the percentage and area calculations. It should be also noted that the difference between the images were presented in Table 4. According to the presented results, when evaluated as a percentage, some classes show negative changes (e.g., water, bare soil and agriculture) and some classes demonstrate positive changes (e.g., road, urban and forest). While the highest decrease was calculated as 8.91% for bare soil class and the highest increase was estimated as 6.08% for forest class. Although the percentage increase of the road class does not seem high, the area of the road class increased considerably almost doubled (Table 4). The reason is that new roads were needed to provide access to the third bridge connection Asia to Europe and the new airport, which is declared as the biggest airport in the world. Besides, urbanization has also been widespread because of the construction of new roads. The LULC analyses as given in Table 4, demonstrating significant decrease of agriculture class from 305.21 km^2 (12.06 % in 2013) to 274.99 km^2 (10.86 % in 2018). Moreover, the water bodies in district of Arnavutkoy were dried up due to the construction of the new airport area. As a result, there was a loss up to 5 km^2 area in water class.

Table 4. The LULC classes of the study area in 2013 and 2018.

LULC Class	2013		2018		Changes (2018-2013)	
	Percent (%)	Area (km^2)	Percent (%)	Area (km^2)	Percent (%)	Area (km^2)
Water	45.70	1,156.87	45.51	1,151.91	-0.19	-4.96
Road	0.88	22.41	1.53	38.77	0.65	16.36
Bare Soil	11.28	285.48	2.37	60.07	-8.91	-225.41
Urban	9.52	240.91	13.09	331.23	3.57	90.32
Forest	20.56	520.32	26.64	674.22	6.08	153.91
Agriculture	12.06	305.21	10.86	274.99	-1.19	-30.22

Table 5 shows obvious changes between LULC classes in the study area. Particularly, the changing areas in the bare soil transformed into urban, forest and agriculture areas. After bare soil class, the most change was observed in the forest class. According to 2013 results, it was observed that area of agriculture class decreased in 2018 with 30.2207 km^2. Also, it can be seen from Table 5 that agriculture class changed into forest and urban class.

Table 5. The changes of LULC classes of study area in 2013 and 2018.

2013	2018	Area (km^2)	Percent (%)	2013	2018	Area (km^2)	Percent (%)
Water	Road	1.16	0.05	Urban	Water	1.33	0.05
Water	Bare Soil	5.12	0.20	Urban	Road	13.39	0.53
Water	Urban	4.79	0.19	Urban	Bare Soil	8.63	0.34
Water	Forest	0.92	0.04	Urban	Forest	34.53	1.36
Water	Agriculture	0.74	0.03	Urban	Agriculture	36.70	1.45
Road	Water	0.37	0.01	Forest	Water	1.16	0.05
Road	Bare Soil	1.63	0.06	Forest	Road	2.96	0.12
Road	Urban	11.30	0.45	Forest	Bare Soil	11.92	0.47
Road	Forest	0.98	0.04	Forest	Urban	30.16	1.19
Road	Agriculture	2.12	0.08	Forest	Agriculture	19.27	0.76
Bare Soil	Water	3.86	0.15	Agriculture	Water	1.07	0.04
Bare Soil	Road	10.19	0.40	Agriculture	Road	5.07	0.20
Bare Soil	Urban	70.34	2.78	Agriculture	Bare Soil	10.88	0.43
Bare Soil	Forest	118.32	4.67	Agriculture	Urban	68.30	2.70
Bare Soil	Agriculture	60.88	2.41	Agriculture	Forest	64.63	2.55

5. CONCLUSION

This study examined the LULC change and land degradation in metropolitan city of Istanbul, which has undergone considerable amount of alterations between 2013 and 2018 due to construction of motorways, bridges and airport. Especially, the region including the construction of the IGA and Yavuz Sultan Selim Bridge was selected as the study area and the changes due to construction were analyzed using multi-temporal satellite images. In this paper, LULC maps of the study area were generated considering the object-based classification employing nearest neighborhood classifier. Six LULC classes comprises namely water, urban, bare soil, forest, agriculture and road classes were used in the object-based classification. In classification process, multiple indices and spectral attributes were utilized. It was observed that the overall accuracies of both LULC maps were produced over 85%. LULC maps were compared for the change detection for a period of five years (2013-2018). Thus, analysis for change areas was conducted for the study area. As a result, a total change of the study covering approximately 24% of the total was observed within five-year. In addition, results showed the highest change occurred in soil class with 225.4149 km^2 and the lowest change occurred in water class with 4.9568 km^2. The five-year change greatly affected the ecosystem of the study area in negative and positive aspects. Specially, the water bodies in the area of the IGA that were previously home for many birds were dried. On the other hand, it was observed that forest area increased in 2018 with 153.9067 km^2 along. In conclusion, although Landsat imagery is not a very high-resolution imagery, these images are found adequate for change detection analysis for this study site.

REFERENCES

Adam, H. E., Csaplovics, E., & Elhaja, M. E., 2016. A comparison of pixel-based and object-based approaches for land use land cover classification in semi-arid areas, Sudan. IOP Conference Series: Earth and Environmental Science, 37.

Anders, N. S., Seijmonsbergen, A. C., & Bouten, W., 2011. Segmentation optimization and stratified object-based analysis for semi-automated geomorphological mapping. Remote Sensing of Environment, 115 (12), pp. 2976–2985.

Boyaci, D., Erdogan, M., & Yildiz, F., 2017. Pixel- versus object-based classification of forest and agricultural areas from multiresolution satellite images. Turkish Journal of Electrical Engineering & Computer Sciences, 25, pp. 365-375.

Chen, G., Hay, J., Carvalho, L., & Wulder, M., 2012. Object-based change detection. International Journal of Remote

Sensing, 33 (14), pp. 4434-4457.
Chen, G., Weng, Q., Hay, G. J., & He, Y., 2018. Geographic object-based image analysis (GEOBIA): Emerging trends and future opportunities. GIScience & Remote Sensing, 55 (2), pp. 159-182.
Definiens, 2007. Developer 7 reference book.
ESRI, n.d. Fundamentals of panchromatic sharpening. Retrieved from http://desktop.arcgis.com/en/arcmap/10.3/manage-data/raster-and-images/fundamentals-of-panchromatic-sharpening.htm#ESRI_SECTION1_F47431B830B24F1D9CD9EF35A256CF9D.
Harris Geospatial, n.d. Atmospheric correction, Retrieved from https://www.harrisgeospatial.com/docs/AtmosphericCorrection.html.
Hussain, M., Chen, D., Cheng, A., Wei, H., & Stanley, D., 2013. Change detection from remotely sensed images: from pixel-based to object-based approaches. ISPRS Journal of Photogrammetry and Remote Sensing, 80, pp. 91-106.
Kavzoglu, T., Erdemir, M. Y., & Tonbul, H., 2016. A region-based multi-scale approach for object-based image analysis. International Archives of the Photogrammetry, Remote Sensing and Spatial Information Sciences, XLI-B7, pp. 241–247.
Kavzoglu, T., Erdemir, M. Y., & Tonbul, H., 2017. Classification of semiurban landscapes from very high-resolution satellite images using a regionalized multiscale segmentation approach. Journal of Applied Remote Sensing, 11(3), 035016.
Kavzoglu, T., Tonbul, H., Erdemir, M., & Colkesen, I., 2018. Dimensionality reduction and classification of hyperspectral images using object-based image analysis. Journal of the Indian Society of Remote Sensing, 46 (8), pp. 1297-1306.
Linli, C., Jun, S., Ping, T., & Huaqiang, D., 2008. Comparison study on the pixel-based and object-oriented methods of land-use/cover classification with TM data. 2008 International Workshop on Earth Observation and Remote Sensing Applications.
Listner, C., & Niemeyer, I., 2011. Object-based change detection. Photogrammetrie - Fernerkundung - Geoinformation, 2011 (4), pp. 233-245.
Ma, L., Li, M., Blaschke, T., Ma, X., Tiede, D., Cheng, L., Chen, D., 2016. Object-based change detection in urban areas: the effects of segmentation strategy, scale, and feature space on unsupervised methods. Remote Sensing, 8 (9), pp. 761.
Myint, S. W., Gober, P., Brazel, A., Grossman-Clarke, S., & Weng, Q., 2011. Per-pixel vs. object-based classification of urban land cover extraction using high spatial resolution imagery. Remote Sensing of Environment, 115 (5), pp. 1145-1161.
NOAA, 2009. What is the difference between land cover and land use, Retrieved Sep 10, 2009, from https://oceanservice.noaa.gov/facts/lclu.html.
Stow, D., Lopez, A., Lippitt, C., Hinton, S., & Weeks, J., 2007. Object-based classification of residential land use within Accra, Ghana based on QuickBird satellite data. International Journal of Remote Sensing, 28 (22), pp. 5167–5173.
Walter, V., 2004. Object-based classification of remote sensing data for change detection. ISPRS Journal of Photogrammetry and Remote Sensing, 58 (3-4), pp. 225-238.
Wu, Y., Ke, Y., Gong, H., Chen, B., & Zhu, L., 2014. Comparison of object-based and pixel-based methods for urban land-use classification from WorldView-2 imagery. 2014 Third International Workshop on Earth Observation and Remote Sensing Applications.